9

Noisy output: escape rate and soft threshold

There are various ways to introduce noise in formal spiking neuron models. In the previous chapter we focused on input noise in the form of stochastic spike arrival. In this chapter we assume that the input is known or can be estimated. Stochasticity arises at the level of the neuronal spike generation, i.e., at the moment of the output. The noisy output can be interpreted as arising from a "soft" threshold that enables an "escape" of the membrane potential across the threshold even before the threshold is reached. Models with a noisy threshold or escape noise are the basis of Generalized Linear Models which will be used in Chapters 10 and 11 as a powerful statistical tool for modeling spike-train data.

In Section 9.1, the notion of escape noise is introduced. In Section 9.2 we determine the likelihood that a specific spike train is generated by a neuron model with escape noise. In Section 9.3 we apply the escape noise formalism to the Spike Response Model already encountered in Chapter 6 and show an interesting link to the renewal statistics encountered in Chapter 7. The escape rate formalism gives rise to an efficient description of noise processes, independently of their biophysical nature, be it channel noise or stochastic spike arrival. Indeed, as shown in Section 9.4, noisy input models and noisy output models can behave rather similarly.

9.1 Escape noise

In the escape noise model, we imagine that an integrate-and-fire neuron with threshold ϑ can fire even though the formal threshold ϑ has not been reached, or may stay quiescent even though the formal threshold has transiently been passed. To do this consistently, we introduce an "escape rate" or "firing intensity" which depends on the momentary state of the neuron.

9.1.1 Escape rate

Given the input $I(t')$ for $t' < t$ and the past firing times $t^f < t$, the membrane potential of a generalized integrate-and-fire model (e.g., the adaptive leaky integrate-and-fire model) or a Spike Response Model (SRM) can be calculated from Eq. (6.7) or Eq. (6.27) respectively;

https://doi.org/10.1017/CBO9781107447615.011 Published online by Cambridge University Press

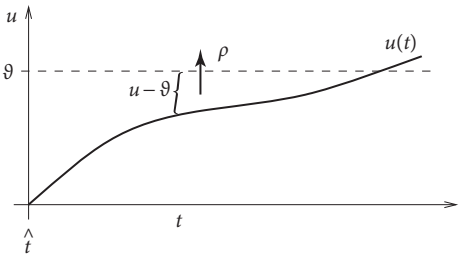

Fig. 9.1 Noisy threshold. A neuron can fire at time t with probability density $\rho(t) = f[u(t) - \vartheta]$ even though the membrane potential u has not yet reached the threshold ϑ. In other words, the sharp threshold of the deterministic neuron is replaced by a "soft" threshold.

see Chapter 6. For example, the value of the membrane potential of an SRM can be expressed as

$$u(t) = \sum_f \eta(t - t^f) + \int_0^\infty \kappa(s)\, I^{\rm det}(t-s)\, {\rm d}s + u_{\rm rest}, \tag{9.1}$$

where $I^{\rm det}$ is the known driving current (the superscript "det" stands for deterministic) and κ and η are filters that describe the response of the membrane to an incoming pulse or an outgoing spike; see Chapter 6. In the deterministic model the next spike occurs when u reaches the threshold ϑ. In order to introduce some variability into the neuronal spike generator, we replace the strict threshold by a stochastic firing criterion. In the noisy threshold model, spikes can occur at any time with a probability density

$$\rho(t) = f(u(t) - \vartheta) \tag{9.2}$$

that depends on the momentary distance between the (noiseless) membrane potential and the threshold; see Fig. 9.1. We can think of f as an escape rate similar to the one encountered in models of chemical reactions (van Kampen, 1992). In the mathematical theory of point processes, the quantity ρ is called a "stochastic intensity." Since we use ρ in the context of neuron models we will refer to it as a firing intensity.

The choice of the escape function f in Eq. (9.2) is arbitrary. A reasonable condition is to require $f \to 0$ for $u \to -\infty$ so that the neuron does not fire if the membrane potential is far below threshold. A common choice is the exponential,

$$f(u - \vartheta) = \frac{1}{\tau_0} \exp[\beta\,(u - \vartheta)]\,, \tag{9.3}$$

where β and τ_0 are parameters. For $\beta \to \infty$, the soft threshold turns into a sharp one so that we return to the noiseless model. Below we discuss some further choices of the escape function in Eq. (9.2).

The SRM of Eq. (9.1) together with the exponential escape rate of Eq. (9.3) is an example of a Generalized Linear Model. Applying the theory of Generalized Linear Mod-

https://doi.org/10.1017/CBO9781107447615.011 Published online by Cambridge University Press

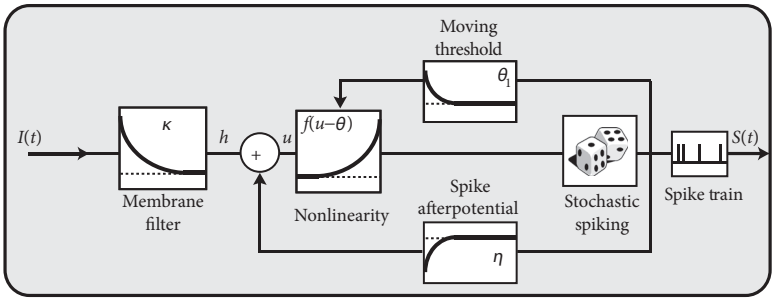

Fig. 9.2 Flow diagram for a Spike Response Model (SRM) with escape noise. The stochasticity at the noisy threshold is indicated by the dice; see Fig. 6.11. The noisy SRM (Gerstner and van Hemmen, 1992; Gerstner and Kistler, 2002) is an example of a Generalized Linear Model (GLM) (Truccolo *et al*., 2005; Pillow *et al*., 2008).

els (see Chapter 10) to the SRM with escape noise enables a rapid extraction of model parameters from experimental data.

In slice experiments it was found (Jolivet *et al*., 2006) that the exponential escape rate of Eq. (9.3) provides an excellent fit to the spiking intensity of real neurons (Fig. 9.3). Moreover, the firing times of an AdEx model driven by a deterministic fluctuating current $I^{\rm det}(t)$ and a unknown white noise current $\xi(t)$ can also be well fitted by the Spike Response Model of Eq. (9.1) combined with an exponential escape rate as we shall see below in Section 9.4.

Nevertheless, we may wonder whether Eq. (9.2) is a sufficiently general noise model. We have seen in Chapter 2 that the concept of a pure voltage threshold is questionable. More generally, the spike trigger process could, for example also depend on the slope $\dot{u} = {\rm d}u/{\rm d}t$ with which the "threshold" is approached. In the noisy threshold model, we may therefore also consider an escape rate (or hazard) which depends not only on u but also on its derivative $\dot{u}$

$$\rho(t) = f[u(t) - \vartheta, \dot{u}(t)]\,. \tag{9.4}$$

We will return to Eq. (9.4) in Section 9.4.

Note that the time dependence of the firing intensity $\rho(t)$ on the right-hand side of Eq. (9.4) arises *implicitly* via the membrane potential $u(t)$. In an even more general model, we could in addition include an *explicit* time dependence, for example, to account for a reduced spiking probability immediately after a spike at t^f. Instead of an explicit dependence, a slightly more convenient way to implement an additional time dependence is via a time-dependent threshold $\vartheta \longrightarrow \vartheta(t)$ which we have already encountered in Eq. (6.31). An even more general escape rate model therefore is

$$\rho(t) = f[u(t) - \vartheta(t), \dot{u}(t)]\,. \tag{9.5}$$

In Chapter 11 we shall see that a Spike Response Model with escape noise and dynamic threshold can explain neuronal firing with a high degree of accuracy.

https://doi.org/10.1017/CBO9781107447615.011 Published online by Cambridge University Press

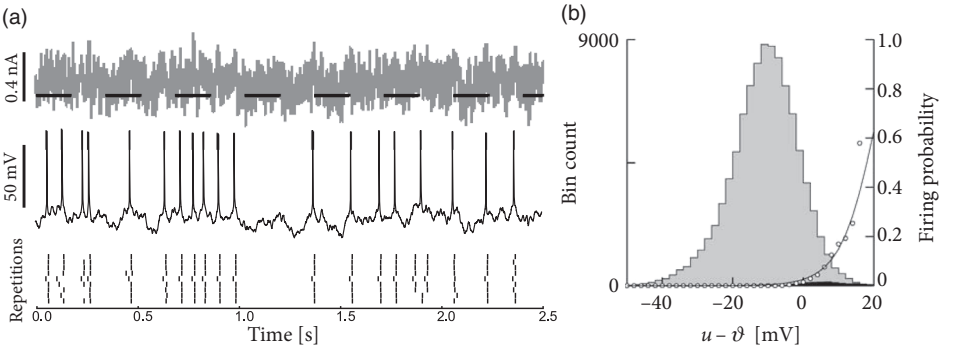

Fig. 9.3 The instantaneous firing intensity extracted from experiments can be fitted by an exponential escape rate. (a) A real neuron is driven by a time-dependent input current (top) generating a fluctuating voltage with occasional spikes (middle), which are repeated with high precision, but not perfectly, across several trials (bottom). (b) The black histogram (very small) shows the number of times (bin count, vertical axis) that the model voltage calculated from Eq. (9.1) falls in the bin $u - \vartheta$ (horizontal axis) *and* the real neuron fires. The gray histogram indicates distribution of voltage when the real neuron does not fire. The ratio (black/black plus gray) in each bin gives the firing probability $P_F(u - \vartheta)$ (open circles, probability scale on the right) which can be fitted by Eq. (9.8) using an exponential escape rate (solid line), $f(u - \vartheta) = \frac{1}{\tau_0} \exp[\beta\,(u - \vartheta)]$ with a steepness of $\beta = (4\,\mathrm{mV})^{-1}$ and a mean latency at threshold of $\tau_0 = 19$ ms. From Jolivet *et al.* (2006) with kind permission from Springer Science and Business Media.

Example: Bounded versus unbounded escape rate

A stochastic intensity which diverges for $u \gg \vartheta$, such as the exponential escape rate of Eq. (9.3), may seem surprising at a first glance, but it is in fact a necessary requirement for the transition from a soft to a sharp threshold process. Since the escape model has been introduced as a noisy threshold, there should be a limit of low noise that leads us back to the sharp threshold. In order to explore the relation between noisy and deterministic threshold models, we consider as a first step a bounded escape function f defined as

$$f(u - \vartheta) = \begin{cases} 0 & \text{for } u < \vartheta, \\ \Delta^{-1} & \text{for } u \geq \vartheta. \end{cases} \tag{9.6}$$

Thus, the neuron never fires if the voltage is below the threshold. If $u > \vartheta$, the neuron fires stochastically with a rate Δ^{-1}. Therefore, the mean latency, or expected delay, of a spike is Δ. This implies that the neuron responds slowly and imprecisely, even when the membrane potential is significantly above threshold – and this result looks rather odd. Only in the limit where the parameter Δ goes to zero would the neuron fire immediately and reliably as soon as the membrane potential crosses the threshold. Thus, a rapid response requires the escape to diverge.

The argument here was based on a step function for the escape rate. A simple choice

https://doi.org/10.1017/CBO9781107447615.011 Published online by Cambridge University Press

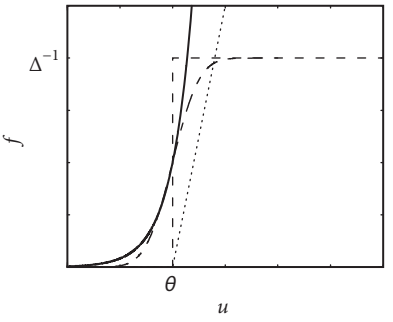

Fig. 9.4 Soft threshold escape rates. Exponential function (solid), piecewise linear function (dotted), step function (dashed), and error function (dot-dashed). The step function and error function saturate at a maximum rate of Δ^{-1}. The threshold is ϑ.

for a soft threshold which enables a rapid response is a piecewise linear escape rate,

$$f(u-\vartheta) = \alpha\,[u-\vartheta]_+ = \begin{cases} 0 & \text{for } u < \vartheta, \\ \alpha\,(u-\vartheta) & \text{for } u \geq \vartheta, \end{cases} \tag{9.7}$$

with slope α for $u > \vartheta$. For $u > \vartheta$, the firing intensity is proportional to $u - \vartheta$; see Fig. 9.4. This corresponds to the intuitive idea that instantaneous firing rates increase with the membrane potential. Variants of the linear escape–rate model are commonly used to describe spike generation in, for example, auditory nerve fibers (Siebert and Gray, 1963; Miller and Mark, 1992).

9.1.2 Transition from continuous time to discrete time

In discrete time, we consider the probability $P_F(u)$ of firing in a finite time step given that the neuron has membrane potential u. It is bounded from above by 1 – despite the fact that the escape rate can be arbitrarily large. We start from a model in continuous time and discretize time as is often done in simulations. In a straightforward discretization scheme, we would calculate the probability of firing during a time step Δt as $\int_t^{t+\Delta t} \rho(t')\mathrm{d}t' \approx \rho(t)\,\Delta t$. However, for $u \gg \vartheta$, the hazard $\rho(t) = f(u(t)-\vartheta)$ can take large values; see, for example, Eq. (9.3). Thus Δt must be taken extremely short so as to guarantee $\rho(t)\,\Delta t < 1$.

To arrive at an improved discretization scheme, we calculate the probability that a neuron does *not* fire in a time step Δt. The probability $S(t)$ of surviving for a time t without firing decays according to $\mathrm{d}S/\mathrm{d}t = -\rho(t)\,S(t)$. Integration of the differential equation over a *finite* time Δt yields an exponential factor $S(t) = \exp[-\int_0^t \rho(t')\,\mathrm{d}t']$; compare the discussion of the survivor function in Chapter 7 (Section 7.5). If the neuron does not survive, it must have fired. Therefore we arrive at a firing probability

$$P_F(u) = \text{Prob}\left\{\text{spike in } [t,t+\Delta t]\,|\,u(t)\right\} \approx 1 - \exp\left\{-\Delta t\, f(u(t)-\vartheta)\right\}. \tag{9.8}$$

Even if f diverges for $u \to \infty$, the probability of firing remains bounded between zero and 1. Also, we see that, for small Δt, the probability P_F scales as $f\Delta t$. We see from Fig. 9.5a that, for an exponential escape rate, an increase in the discretization Δt mainly shifts the

https://doi.org/10.1017/CBO9781107447615.011 Published online by Cambridge University Press

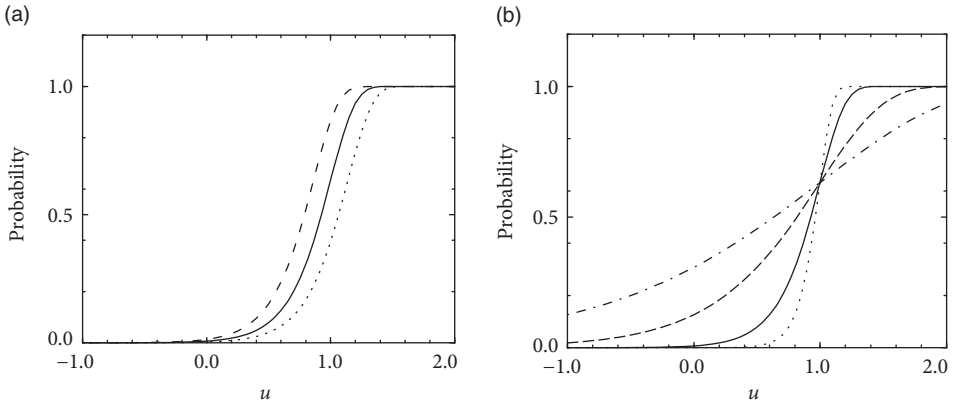

Fig. 9.5 The unbounded exponential escape rate yields a bounded firing probability in a discrete time step. (a) Probability of firing in a discrete time interval Δt as a function of the membrane potential u for different discretizations $\Delta t = 0.5$ ms (dashed line), $\Delta t = 1$ ms (solid line), and $\Delta t = 2$ ms (dotted line) with $\beta = 5$. (b) Similar plot as in A but for different noise levels $\beta = 10$ (dotted line), $\beta = 5$ (solid line), $\beta = 2$ (dashed line), and $\beta = 1$ (dot-dashed line) with $\Delta t = 1$ ms. The escape rate is given by (9.3) with parameters $\vartheta = 1$ and $\tau_0 = 1$ ms.

firing curve to the left while the form remains roughly the same. An increase of the noise level makes the curve flatter; see Fig. 9.5b.

Note that, because of refractoriness, it is impossible for integrate-and-fire models (and for real neurons) to fire more than one spike in a short time bin Δt. Refractoriness is implemented in the model of Eq. (9.1) by a significant reset of the membrane potential via the refractory kernel η.

9.2 Likelihood of a spike train

In the previous subsection, we calculated the probability of firing in a short time step Δt from the continuous-time firing intensity $\rho(t)$. Here we ask a similar question, not on the level of a single spike, but on that of a full spike train.

Suppose we know that a spike train has been generated by an escape noise process

$$\rho(t) = f(u(t) - \vartheta) \tag{9.9}$$

as in Eq. (9.2), where the membrane potential $u(t)$ arises from the dynamics of one of the generalized integrate-and-fire models such as the SRM.

The likelihood L^n that spikes occur at the times $t^1, \dots, t^f, \dots, t^n$ is (Brillinger, 1988)

$$L^n(\{t^1, t^2, \dots, t^n\}) = \rho(t^1) \cdot \rho(t^2) \cdot \dots \rho(t^n) \exp\left[-\int_0^T \rho(s) \mathrm{d}s\right], \tag{9.10}$$

where $[0, T]$ is the observation interval. The product on the right-hand side contains the momentary firing intensity $\rho(t^f)$ at the firing times $t^1, t^2, \dots, t^n$. The exponential factor

https://doi.org/10.1017/CBO9781107447615.011 Published online by Cambridge University Press

takes into account that the neuron needs to "survive" without firing in the intervals between the spikes.

In order to highlight this interpretation it is convenient to take a look at Fig. 9.6a and rewrite Eq. (9.10) in the equivalent form

$$\begin{aligned} L^n(\{t^1,t^2,\dots,t^n\}) = \exp\left[-\int_0^{t^1}\rho(s)\mathrm{d}s\right] \\ \cdot\rho(t^1)\quad \exp\left[-\int_{t^1}^{t^2}\rho(s)\mathrm{d}s\right] \\ \cdot\rho(t^2)\quad \exp\left[-\int_{t^2}^{t^3}\rho(s)\mathrm{d}s\right] \\ \cdot\dots\rho(t^n)\quad \exp\left[-\int_{t^n}^{T}\rho(s)\mathrm{d}s\right]. \end{aligned} \tag{9.11}$$

Intuitively speaking, the likelihood of finding n spikes at times t^f depends on the instantaneous rate at the time of the spikes and the probability of surviving the intervals in between without firing; see the survivor function introduced in Chapter 7, Eq. (7.26).

Instead of the likelihood, it is sometimes more convenient to work with the logarithm of the likelihood, called the log-likelihood

$$\log L^n(\{t^1,\dots,t^f,\dots,t^n\}) = -\int_0^T \rho(s)\mathrm{d}s + \sum_{f=1}^{n}\log\rho(t^f). \tag{9.12}$$

The three formulations Eqs. (9.10)–(9.12) are equivalent and it is a matter of taste if one is preferred over the others.

Example: Discrete-time version of likelihood and generative model

In a discrete-time simulation of an SRM or generalized integrate-and-fire model with escape noise, we divide the simulation interval $[0,T]$ into N time steps $\Delta t = T/N$; see Fig. 9.6b. In each time step, we first calculate the membrane potential $u(t)$ and then generate a spike with probability $P_t = P_F(u(t))$ given by Eq. (9.8). To do so, we generate on the computer a random number r_t between zero and unity. If $P_t > r_t$, a spike is generated, i.e., the spike count number in this time bin is $n_t = 1$. The probability of finding an empty time bin (spike count $n_t = 0$) is

$$\mathrm{Prob}\{\text{silent in } [t,t+\Delta t]\} = 1 - P_t = \exp\{-\Delta t\,\rho(t)\}\,, \tag{9.13}$$

where we have assumed that time bins are short enough so that the membrane potential does not change a lot from one time step to the next. The spike train can be summarized as a binary sequence $\{0,0,1,0,0,0,1,0,\dots\}$ of N numbers $n_t \in \{0,1\}$. We emphasize that, with the above discrete-time spike generation model, it is impossible to have two spikes in a time bin Δt. This reflects the fact that, because of neuronal refractoriness,

https://doi.org/10.1017/CBO9781107447615.011 Published online by Cambridge University Press

neurons cannot emit two spikes in a time bin shorter than, say, half the duration of an action potential.

Since we generate an independent random number in each time bin, a specific spike train occurs with a probability given by the product of the probabilities per bin:

$$P_{\text{total}} = \Pi_{\text{bins with spike}}[P_t] \cdot \Pi_{\text{empty bins}}[1-P_t] \tag{9.14}$$

$$= \Pi_t \left\{ [P_t]^{n_t} \cdot [1-P_t]^{1-n_t} \right\}, \tag{9.15}$$

where the product runs over all time bins and $n_t \in \{0,1\}$ is the spike count number in each bin.

We now switch our perspective and study an *observed* spike train in continuous time with spike firings at times t^f with $0 < t^1, t^2, \ldots, t^n < T$. The spike train was generated by a real neuron in a slice experiment under current injection with a known current $I(t)$. We now ask the following question: What is the probability that the observed spike train *could have been generated* by our model? Thus, we consider our discrete-time model with escape noise as a *generative* model of the spike train. To do so, we calculate the voltage using a discrete-time version of Eq. (9.1). Given the (known) injected input $I(t)$ and the (observed) spike times t^f, we can calculate the voltage $u(t)$ of our model and therefore the probability of firing in each time step.

The observed spike train has n spikes at times $0 < t^1, t^2, \ldots, t^n < T$. Let us denote time bins containing a spike by t_k with index k (i.e., $t_1 < t^1 \leq t_1 + \Delta t$; $t_2 < t^2 \leq t_2 + \Delta t$; $\ldots$) and empty bins by $t_{k'}$ with a dummy index k'. Using Eq. (9.14), the probability that the observed spike train could have been generated by our model is

$$P_{\text{total}} = \Pi_{k=1}^{n}[P_{t_k}] \cdot \Pi_{k', t_{k'} \neq t_k}[1-P_{t_{k'}}]. \tag{9.16}$$

Eq. (9.16) is the starting point for finding optimal parameters of neuron models (Chapter 10).

We can gain some additional insights, if we rearrange the terms on the right-hand side of Eq. (9.16) differently. All time bins that fall into the interval *between* two spikes can be regrouped as follows

$$\Pi_{\{k'|t_k<t_{k'}\leq t_{k+1}\}}[1-P_{t_{k'}}] = \Pi_{\{k'|t_k<t_{k'}\leq t_{k+1}\}} \exp\{-\Delta t\, \rho(t_{k'})\}$$

$$= \exp\left\{ - \sum_{t_k < t_{k'} < t_{k+1}} \Delta t\, \rho(t_{k'}) \right\}. \tag{9.17}$$

Ideally, a spike train in continuous time should be described by a model in continuous time. We therefore ask whether the discretization of time is critical or whether we can get rid of it. The transition to continuous time corresponds to the limit of $N \to \infty$ while T is kept fixed. The Riemann sum on the right-hand side of Eq. (9.17) then turns into an integral. In the same limit, the contribution of the bins containing a spike to Eq. (9.16) can be written as $P_{t_k} = \rho(t_k)\Delta t$. We are led back from the discrete-time generative model

https://doi.org/10.1017/CBO9781107447615.011 Published online by Cambridge University Press

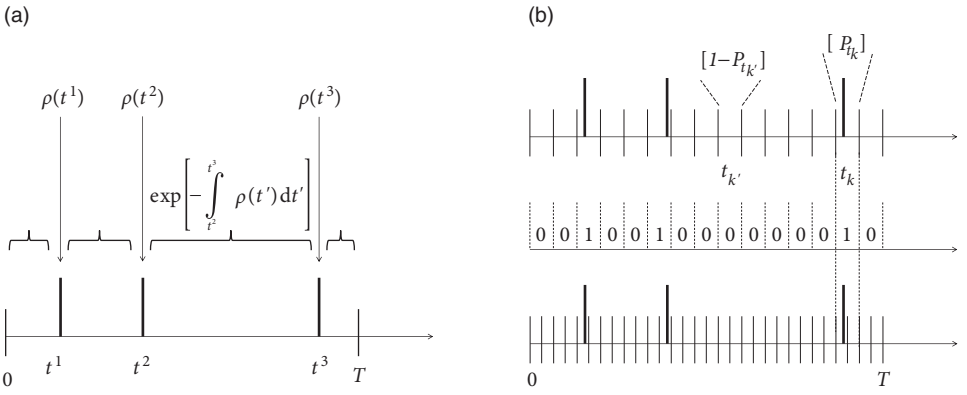

Fig. 9.6 Likelihood of a spike train. Three spikes (thick vertical lines) have been observed in the interval $[0,T]$. (a) The instantaneous firing rates at the moment of the spikes are $\rho(t^1),\rho(t^2),\rho(t^3)$, respectively. The intervals without spike firing are indicated by horizontal braces. The probability of staying quiescent during these intervals decays exponentially with the time-dependent rate $\rho(t')$. (b) Likelihood of a spike train in discrete time. Top: The probability that a time bin $t_{k'}$ contains no spike is $1-P_{t_{k'}}$ whereas the probability that a spike occurs in bin t_k is P_{t_k}. Middle: The spike count numbers $n_t \in \{0,1\}$ in each time bin. Bottom: The same spike train can also be described using a finer time discretization.

to Eq. (9.11) in continuous time with the replacement

$$P_{\text{total}} = L^n(\{t^1,t^2,\dots t^n\})(\Delta t)^n, \tag{9.18}$$

i.e., the continuum limit exists. In other words, once the time steps Δt are short enough, the exact discretization scheme does not play a role. Alternative, more efficient, sampling schemes exist that avoid discretization (Brown *et al.*, 2002); see Section 10.3.3.

9.3 Renewal approximation of the Spike Response Model

We focus on a Spike Response Model with escape noise; see Eqs. (9.1)–(9.3). If the firing rate is low, so that the interspike interval is much longer than the decay time of the refractory kernel η, then we can truncate the sum over past firing times and keep track only of the effect of the most recent spike (Gerstner, 1995)

$$u(t) = \eta(t-\hat{t}) + \int_0^\infty \kappa(s)\, I^{\text{det}}(t-s)\,ds + u_{\text{rest}}, \tag{9.19}$$

where $\hat{t}$ denotes the *last* firing time $t^f < t$.

Eq. (9.19) is called the "short-term memory" approximation of the SRM and abbreviated as SRM_0. This model can be efficiently fitted to neural data (Kass and Ventura, 2001) and will play an important role in Chapter 14. In order to emphasize that the value of the membrane potential depends only on the most recent spike, in what follows we write $u(t|\hat{t})$

https://doi.org/10.1017/CBO9781107447615.011 Published online by Cambridge University Press

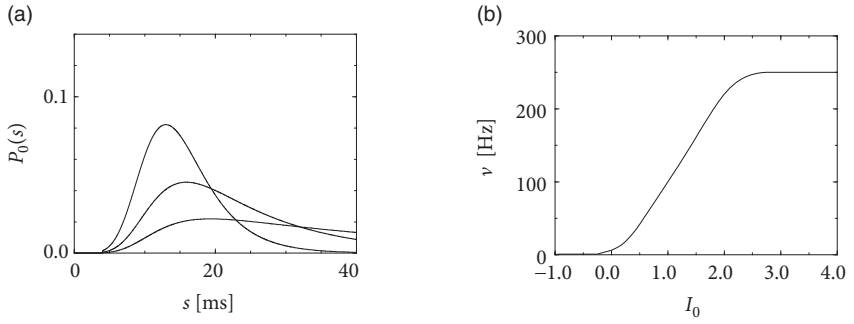

Fig. 9.7 (a) Interval distribution $P_0(s)$ for an SRM_0 neuron with absolute refractory period $\Delta^{\mathrm{abs}} = 4\,\mathrm{ms}$ followed by an exponentially decreasing afterpotential as in Eq. (9.24) with $\eta_0 = 1$ and $\tau = 4\,\mathrm{ms}$. The model neuron is stimulated by a constant current $I_0 = 0.7, 0.5, 0.3$ (from top to bottom). (b) Output rate ν as a function of I_0 (gain function). The escape rate is given by Eq. (9.3) with $\vartheta = 1$, $\beta = 5$, and $\tau_0 = 1\,\mathrm{ms}$.

instead of $u(t)$. Let us summarize the total effect of the input by introducing the "input potential"

$$h(t) = \int_0^\infty \kappa(s)\, I^{\mathrm{det}}(t-s)\, \mathrm{d}s, \tag{9.20}$$

which allows us to rewrite Eq. (9.19) as

$$u(t|\hat{t}) = \eta(t-\hat{t}) + h(t) + u_{\mathrm{rest}}\,. \tag{9.21}$$

The escape rate

$$\rho(t|\hat{t}) = f(u(t|\hat{t})) \tag{9.22}$$

depends on the time since the last spike and, implicitly, on the stimulating current $I_{\mathrm{det}}(t)$. Hence $\rho(t|\hat{t})$ is similar to the hazard variable of stationary renewal theory. The arguments of Chapter 7 can be generalized to the case of time-dependent input $I^{\mathrm{det}}(t)$ which gives rise to a time-dependent input potential $h(t)$. Given that the neuron has fired its last spike at time $\hat{t}$ and that we know the input $I^{\mathrm{det}}(t')$ for $t' < t$ we can calculate the probability density that the next spike occurs at time $t > \hat{t}$

$$P_I(t|\hat{t}) = \rho(t|\hat{t}) \exp\left[-\int_{\hat{t}}^{t} \rho(t'|\hat{t})\, \mathrm{d}t'\right]. \tag{9.23}$$

Eq. (9.23) generalizes renewal theory to the time-dependent case. Time-dependent renewal theory will play an important role in Chapter 14.

Compared to the standard stationary renewal theory discussed in Chapter 7, there are two important differences. First, the Spike Response Model with escape noise provides a direct path from stationary to time-dependent renewal theory. Second, interval distributions can be linked to refractoriness and vice versa. More precisely, a reduced firing intensity $\rho(t|\hat{t})$ immediately after a spike is an indication that the distance between the membrane

https://doi.org/10.1017/CBO9781107447615.011 Published online by Cambridge University Press

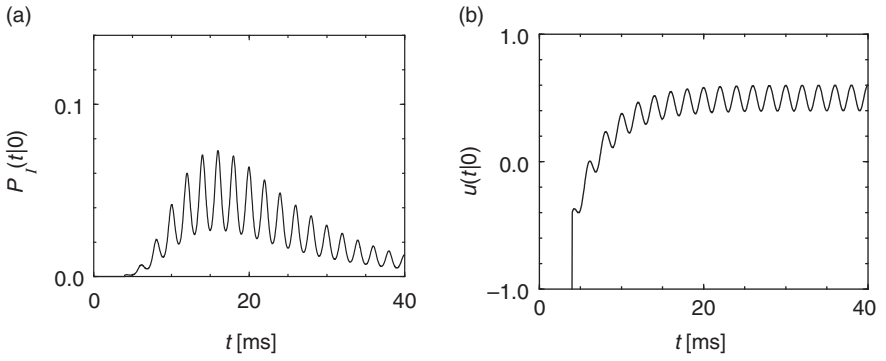

Fig. 9.8 (a) Input-dependent interval distribution $P_I(t|0)$ for an SRM$_0$ neuron as in Fig. 9.7 stimulated by a periodically modulated input field $h(t) = h_0 + h_1 \cos(2\pi f t)$ with $h_0 = 0.5$, $h_1 = 0.1$, and frequency $f = 500$ Hz. (b) The membrane potential $u(t|0) = \eta(t) + h(t)$ during stimulation as in (a).

potential $u(t|\hat{t})$ and the threshold is increased. The reason can be either a hyperpolarizing spike-afterpotential $\eta(t)$ or an increase in the firing threshold $\vartheta(t|\hat{t})$ immediately after a spike

Example: Interval distribution with exponential escape noise

We study a model SRM$_0$ with membrane potential $u(t|\hat{t}) = \eta(t-\hat{t}) + h(t)$ and choose a refractory kernel with absolute and relative refractoriness defined as

$$\eta(s) = \begin{cases} -\infty & \text{for } s < \Delta^{\text{abs}}, \\ -\eta_0 \exp\left(-\frac{s-\Delta^{\text{abs}}}{\tau}\right) & \text{for } s > \Delta^{\text{abs}}. \end{cases} \tag{9.24}$$

We adopt the exponential escape rate (9.3).

Fig. 9.7 shows the interval distribution for constant input current I_0 as a function of $s = t - \hat{t}$. With the normalization $\int_0^\infty \kappa(s)\mathrm{d}s = 1$, we have $h_0 = I_0$. Owing to the refractory term η, extremely short intervals are impossible and the maximum of the interval distribution occurs at some finite value of s. If I_0 is increased, the maximum is shifted to the left. The interval distributions of Fig. 9.7a have qualitatively the same shape as those found for cortical neurons. The gain function $\nu = g(I_0)$ of a noisy SRM$_0$ neuron is shown in Fig. 9.7b.

We now study the same model with periodic input $I^{\text{det}}(t) = I_0 + I_1 \cos(\Omega t)$. This leads to an input potential $h(t) = h_0 + h_1 \cos(\Omega t + \varphi_1)$ with bias $h_0 = I_0$ and a periodic component with a certain amplitude h_1 and phase φ_1.

Suppose that a spike has occurred at $\hat{t} = 0$. The probability density that the next spike occurs at time t is given by $P_I(t|\hat{t})$ and can be calculated from Eq. (9.23). The result is shown in Fig. 9.8a.

https://doi.org/10.1017/CBO9781107447615.011 Published online by Cambridge University Press

We note that the periodic component of the input is well represented in the response of the neuron. This example illustrates how neurons in the auditory system can transmit stimuli of frequencies higher than the mean firing rate of the neuron. We emphasize that the threshold in Fig. 9.8b is at $\vartheta = 1$. Without noise there would be no output spike. On the other hand, at very high noise levels, the modulation of the interval distribution would be much weaker. Thus a certain amount of noise is beneficial for signal transmission. The existence of an optimal noise level is a phenomenon called stochastic resonance and will be discussed below in Section 9.4.2.

9.4 From noisy inputs to escape noise

The total input current $I(t)$ which drives a neuron can often be separated into a deterministic component $I^{\rm det}$, which is known and repeats between one trial and the next; and a stochastic component ξ which is unknown and potentially changes between trials:

$$I(t) = I^{\rm det}(t) + \xi(t)\,. \tag{9.25}$$

In this section we show that the noisy, unknown part in the input can be approximated to a high degree of accuracy by an appropriately chosen escape function.

Example: Adaptive exponential integrate-and-fire model with noisy input

Suppose that the AdEx model which we encountered in Chapter 6 (see Eqs. (6.3) and (6.4)) is driven by an input as in Eq. (9.25) containing a rapidly moving deterministic signal $I^{\rm det}(t)$ as well as a white noise component $\xi(t)$. This model generates spikes with a millisecond precision and a high degree of reliability from one trial to the next (Fig. 9.9). We now approximate the voltage of the AdEx model by a linear model

$$u(t) = \sum_f \eta(t - t_i^f) + \int_0^\infty \kappa(s)\, I^{\rm det}(t-s)\, {\rm d}s + u_{\rm rest}\,. \tag{9.26}$$

In the subthreshold regime $u < \vartheta - \Delta_T$, the filters κ and η can be calculated analytically using the methods discussed in Chapter 6. The voltage equation (9.26) is then combined with the exponential escape rate

$$f(u-\vartheta) = \frac{1}{\tau_0} \exp[\beta\,(u-\vartheta)]\,. \tag{9.27}$$

The resulting SRM with escape noise (i.e., a linear model with exponential soft-threshold noise in the output) describes the activity of the AdEx with noisy input (i.e., an exponential neuron model with additive white noise in the input) surprisingly well (Fig. 9.9). In other words, in the presence of an input noise $\xi(t)$ the exponential term in the voltage equation of the AdEx model can be replaced by an exponential escape rate (Mensi *et al.*, 2011).

https://doi.org/10.1017/CBO9781107447615.011 Published online by Cambridge University Press

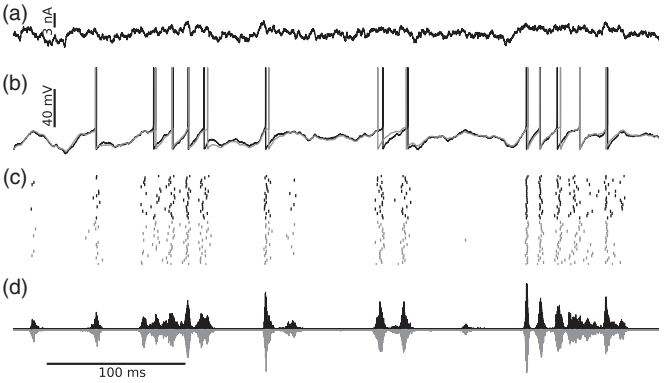

Fig. 9.9 From input noise to output noise. (a) An AdEx model neuron is driven by a fluctuating current containing a deterministic part which is the same during each trial and a stochastic white noise part. (b) Voltage trace of the AdEx model (black) and the SRM with exponential escape rate (gray) during a single trial. The SRM is driven by the determinstic part of the input current. (c) Spike times during 20 trials with the same determinstic current for the AdEx model (black) and SRM with exponential escape noise (gray). For the AdEx the stochasticity arises from white noise in the input whereas for the SRM it arises from escape noise in the output. (d) Comparison of the PSTH of the AdEx model (black) with that of the SRM (gray). Adapted from Mensi *et al*. (2011).

9.4.1 Leaky integrate-and-fire model with noisy input

In the subthreshold regime, the leaky integrate-and-fire model with stochastic input (white noise) can be mapped approximately onto an escape noise model with a certain escape rate f (Plesser and Gerstner, 2000). In this section, we motivate the mapping and the choice of f.

In the absence of a threshold, the membrane potential of an integrate-and-fire model has a Gaussian probability distribution around the noise-free reference trajectory $u_0(t)$. If we take the threshold into account, the probability density at $u = \vartheta$ of the exact solution vanishes, since the threshold acts as an absorbing boundary; see Eq. (8.44). Nevertheless, in a phenomenological model, we can approximate the probability density near $u = \vartheta$ by the "free" distribution (i.e., without the threshold)

$$\text{Prob}\{u \text{ reaches } \vartheta \text{ in } [t, t+\Delta t]\} \propto \Delta t \, \exp\left\{ -\frac{[u_0(t) - \vartheta]^2}{2\langle \Delta u^2(t) \rangle} \right\}, \tag{9.28}$$

where $u_0(t)$ is the noise-free reference trajectory. The idea is illustrated in Fig. 9.10. We note that in a leaky integrate-and-fire model with colored noise (as opposed to white noise) in the input the density at threshold is *not* zero.

We have seen in Eq. (8.13) that the variance $\langle \Delta u^2(t) \rangle$ of the free distribution rapidly approaches a constant value $\sigma^2/2$ where σ scales with the strength of the diffusive input. We therefore replace the time-dependent variance $2\langle \Delta u(t)^2 \rangle$ by its stationary value σ^2. The

https://doi.org/10.1017/CBO9781107447615.011 Published online by Cambridge University Press

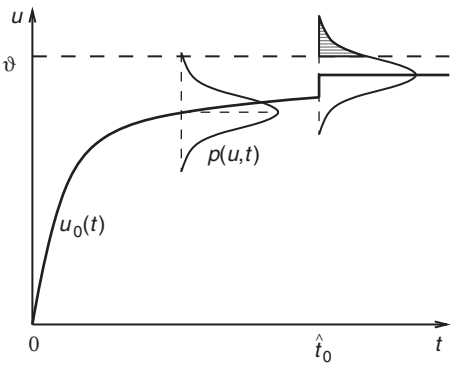

Fig. 9.10 The distribution of the membrane potential around the noise-free reference trajectory $u_0(t)$ is given by $p(u,t)$. At $t = t_0$, where the reference trajectory has a discontinuity, the distribution of the membrane potential is shifted instantaneously across the threshold. The probability of firing at t_0 is given by the shaded surface under the distribution.

right-hand side of Eq. (9.28) is then a function of the noise-free reference trajectory only. To transform the left-hand side of Eq. (9.28) into an escape rate, we divide both sides by Δt. The firing intensity is thus

$$f(u_0 - \vartheta) = \frac{c_1}{\tau_m} \exp\left\{ -\frac{[u_0(t) - \vartheta]^2}{\sigma^2} \right\} . \tag{9.29}$$

The factor in front of the exponential has been split into a constant parameter $c_1 > 0$ and the time constant τ_m of the neuron in order to show that the escape rate has units of 1 over time. Equation (9.29) is the well-known Arrhenius formula for escape across a barrier of height $(\vartheta - u_0)^2$ in the presence of thermal energy σ^2 (van Kampen, 1992).

Let us now suppose that the neuron receives, at $t = t_0$, an input current pulse which causes a jump of the membrane trajectory by an amount $\Delta u > 0$; see Fig. 9.10. In this case the Gaussian distribution of membrane potentials is shifted *instantaneously* across the threshold so that there is a nonzero probability that the neuron fires exactly at t_0. In other words, the firing intensity $\rho(t) = f[u_0(t) - \vartheta]$ has a δ peak at $t = t_0$. The escape rate of Eq. (9.29), however, cannot reproduce this δ peak. More generally, whenever the noise-free reference trajectory increases with slope $\dot{u}_0 > 0$, we expect an increase of the instantaneous rate proportional to $\dot{u}_0$, because the tail of the Gaussian distribution drifts across the threshold; see Eq. (8.35). In order to take the drift into account, we generalize Eq. (9.29) and study

$$f(u_0, \dot{u}_0) = \left(\frac{c_1}{\tau_m} + \frac{c_2}{\sigma} [\dot{u}_0]_+ \right) \exp\left\{ -\frac{[u_0(t) - \vartheta]^2}{\sigma^2} \right\} , \tag{9.30}$$

where $\dot{u}_0 = \mathrm{d}u_0/\mathrm{d}t$ and $[x]_+ = x$ for $x > 0$ and zero otherwise. We call Eq. (9.30) the Arrhenius&Current model (Plesser and Gerstner, 2000).

https://doi.org/10.1017/CBO9781107447615.011 Published online by Cambridge University Press

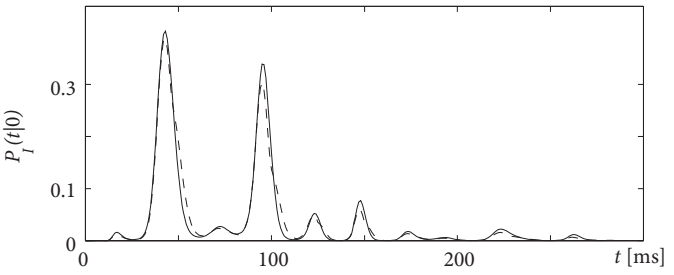

Fig. 9.11 The interval distributions $P_I(t|0)$ for diffusive noise (solid line) and Arrhenius&Current escape noise (dashed line) are nearly identical. The input potential is the same as in Fig. 8.10. Taken from Plesser and Gerstner (2000).

We emphasize that the right-hand side of Eq. (9.30) depends only on the dimensionless variable

$$x(t) = \frac{u_0(t) - \vartheta}{\sigma} \tag{9.31}$$

and its derivative $\dot{x}$. Thus the amplitude of the fluctuations σ define a "natural" voltage scale. The only relevant variable is the momentary distance of the noise-free trajectory from the threshold in units of the noise amplitude σ. A value of $x = -1$ implies that the membrane potential is one σ below threshold. A distance of $u - \vartheta = -10\,\text{mV}$ at high noise (e.g., $\sigma = 10\,\text{mV}$) is as effective in firing a cell as a distance of 1 mV at low noise ($\sigma = 1\,\text{mV}$).

Example: Comparison of diffusion model and Arrhenius&Current escape rate

To check the validity of the arguments that led to Eq. (9.30), let us compare the interval distribution generated by the diffusion model with that generated by the Arrhenius&Current escape model. We use the same input potential $u_0(t)$ as in Fig. 8.10. We find that the interval distribution for the diffusive white noise model (derived from stochastic spike arrival; see Chapter 8) and that for the Arrhenius&Current escape model are nearly identical; see Fig. 9.11. Thus the Arrhenius&Current escape model yields an excellent approximation to the diffusive noise model.

Even though the Arrhenius&Current model has been designed for subthreshold stimuli, it also works remarkably well for superthreshold stimuli. An obvious shortcoming of the escape rate (9.30) is that the instantaneous rate decreases with u for $u > \vartheta$. The superthreshold behavior can be corrected if we replace the Gaussian $\exp(-x^2)$ by $2\exp(-x^2)/[1 + \text{erf}(-x)]$ (Herrmann and Gerstner, 2001). The subthreshold behavior remains unchanged compared to Eq. (9.30) but the superthreshold behavior of the escape rate f becomes linear.

https://doi.org/10.1017/CBO9781107447615.011 Published online by Cambridge University Press

9.4.2 Stochastic resonance

Noise can – under certain circumstances – improve the signal transmission properties of neuronal systems. In most cases there is an optimum for the noise amplitude which has motivated the name *stochastic resonance* for this rather counterintuitive phenomenon. In this section we discuss stochastic resonance in the context of noisy spiking neurons.

We study the relation between an input $I(t)$ to a neuron and the corresponding output spike train $S(t) = \sum_f \delta(t - t^f)$. In the absence of noise, a subthreshold stimulus $I(t)$ does not generate action potentials so that no information on the temporal structure of the stimulus can be transmitted. In the presence of noise, however, spikes do occur. As we have seen in Eq. (9.30), spike firing is most likely at moments when the normalized distance $|x| = |(u - \vartheta)/\sigma|$ between the membrane potential and the threshold is small. Since the escape rate in Eq. (9.30) depends exponentially on x^2, any variation in the membrane potential $u_0(t)$ that is generated by the temporal structure of the input is enhanced; see Fig. 9.8. On the other hand, for very large noise ($\sigma \to \infty$), we have $x^2 \to 0$, and spike firing occurs at a constant rate, irrespective of the temporal structure of the input. We conclude that there is some intermediate noise level where signal transmission is optimal.

The optimal noise level can be found by plotting the signal-to-noise ratio as a function of noise. Even though stochastic resonance does not require periodicity (see, e.g., Collins *et al.*, 1996), it is typically studied with a periodic input signal such as

$$I^{\rm det}(t) = I_0 + I_1 \cos(\Omega t)\,. \tag{9.32}$$

For $t - \hat{t} \gg \tau_m$, the membrane potential of the noise-free reference trajectory has the form

$$u_0(t) = u_\infty + u_1 \cos(\Omega t + \varphi_1)\,, \tag{9.33}$$

where u_1 and φ_1 are the amplitude and phase of its periodic component. To quantify the signal transmission properties, a long spike train is studied and the signal-to-noise ratio (SNR) is computed. The signal $\mathscr{S}$ is measured as the amplitude of the power spectral density of the spike train evaluated at frequency Ω, i.e., $\mathscr{S} = \mathscr{P}(\Omega)$. The noise level $\mathscr{N}$ is usually estimated from the noise power $\mathscr{P}_{\rm Poisson}$ of a Poisson process with the same number of spikes as the measured spike train, i.e., $\mathscr{N} = \mathscr{P}_{\rm Poisson}$. Figure 9.12 shows the signal-to-noise ratio $\mathscr{S}/\mathscr{N}$ of a periodically stimulated integrate-and-fire neuron as a function of the noise level σ. Two models are shown, namely, diffusive noise (solid line) and escape noise with the Arrhenius&Current escape rate (dashed line). The two curves are rather similar and exhibit a peak at

$$\sigma^{\rm opt} \approx \frac{2}{3}\,(\vartheta - u_\infty)\,. \tag{9.34}$$

Since $\sigma^2 = 2\langle \Delta u^2 \rangle$ and $\sqrt{2}\cdot 2/3 \approx 1$, signal transmission is optimal if the stochastic fluctuations of the membrane potential have an amplitude

$$2\sqrt{\langle \Delta u^2 \rangle} \approx \vartheta - u_\infty\,. \tag{9.35}$$

https://doi.org/10.1017/CBO9781107447615.011 Published online by Cambridge University Press

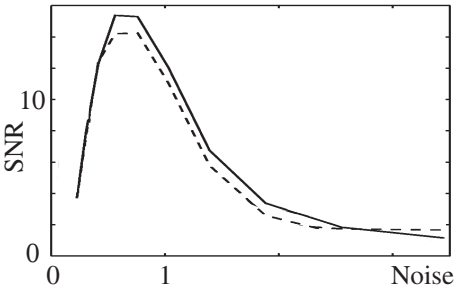

Fig. 9.12 Signal-to-noise ratio (SNR) for the transmission of a periodic signal as a function of the noise level $\sigma/(\vartheta - u_0)$. Solid line: Diffusion model. Dashed line: Arrhenius&Current escape model. Taken from Plesser and Gerstner (2000).

An optimality condition similar to (9.34) holds over a wide variety of stimulation parameters (Plesser, 1999). We will come back to the signal transmission properties of noisy spiking neurons in Chapter 15.

Example: Extracting oscillations

The optimality condition (9.34) can be fulfilled by adapting either the left-hand side or the right-hand side of the equation. Even though it cannot be excluded that a neuron changes its noise level so as to optimize the left-hand side of Eq. (9.34) this does not seem very likely. On the other hand, it is easy to imagine a mechanism that optimizes the right-hand side of Eq. (9.34). For example, an adaptation current could change the value of ϑ, or synaptic weights could be increased or decreased so that the mean potential u_∞ is in the appropriate regime.

We apply the idea of an optimal threshold to a problem of neural coding. More specifically, we study the question of whether an integrate-and-fire neuron or an SRM neuron is sensitive only to the total number of spikes that arrive in some time window T, or also to the relative timing of the input spikes. To do so, we compare two different scenarios of stimulation. In the first scenario, input spikes arrive with a periodically modulated rate,

$$\nu^{\rm in}(t) = \nu_0 + \nu_1 \cos(\Omega t) \tag{9.36}$$

with $0 < \nu_1 < \nu_0$. Thus, even though input spikes arrive stochastically, they have some inherent temporal structure, since they are generated by an *inhomogeneous* Poisson process. In the second scenario, input spikes are generated by a homogeneous (that is, stationary) Poisson process with constant rate ν_0. In a large interval $T \gg \Omega^{-1}$, however, we expect in both cases a total number of $\nu_0 T$ input spikes.

Stochastic spike arrival leads to a fluctuating membrane potential with variance $\Delta^2 = \langle \Delta u^2 \rangle$. If the membrane potential hits the threshold an output spike is emitted. If stimulus

https://doi.org/10.1017/CBO9781107447615.011 Published online by Cambridge University Press

1 is applied during the time T, the neuron emits a certain number of action potentials, say $n^{(1)}$. If stimulus 2 is applied it emits $n^{(2)}$ spikes. It is found that the spike count numbers $n^{(1)}$ and $n^{(2)}$ are significantly different if the threshold is in the range

$$u_\infty + \sqrt{\langle \Delta u^2 \rangle} < \vartheta < u_\infty + 3\sqrt{\langle \Delta u^2 \rangle}\,. \tag{9.37}$$

We conclude that a neuron in the subthreshold regime is capable of transforming a temporal code (amplitude ν_1 of the variations in the input) into a spike count code (Kempter *et al*., 1998). Such a transformation plays an important role in the auditory pathway (Miller and Mark, 1992; Konishi, 1993; Kempter *et al*., 1999b).

9.5 Summary

Neuronal noise in the output can be described as a stochastic firing intensity, or escape rate, which depends on the momentary distance of the membrane potential from the threshold. The concept of escape rate can be applied to a large class of generalized integrate-and-fire models. An SRM with exponential escape rate is particularly attractive for several reasons. First, experimental data suggest an exponential escape rate (Fig. 9.3). Second, a wide spectrum of subthreshold effects can be captured by the linear filters of the SRM (Chapter 6). Third, when driven with a noisy input, nonlinear neuron models such as the AdEx can be well approximated by the SRM with exponential escape noise (Fig. 9.9). Fourth, the explicit formulas for the likelihood of an observed spike train (Section 9.2) enable a rapid fit of the neuron model to experimental data, using the concept of Generalized Linear Models to be discussed in the next chapter.

Escape noise gives rise to variability in spike firing even if the input is perfectly known. It can therefore be linked to intrinsic noise sources such as channel noise. However, more generally, any unknown component of the input which may, for example, arise from stochastic spike arrival can also be approximated by an appropriate escape rate function (Section 9.4). Thus the escape rate provides a phenomenological noise model that summarizes effects of biophysical channel noise as well as stochastic input.

Literature

The Spike Response Model with exponential escape noise was introduced in Gerstner and van Hemmen (1992) and Gerstner (1995), but closely related models had already been applied to neuronal data by Brillinger (1988) and have an obvious link to Generalized Linear Models, which were used in statistics as early as the 1970s (Nelder and Wederburn, 1972) and have been repeatedly applied to neuronal data (Truccolo *et al*., 2005; Pillow *et al*., 2008). The choice of an exponential escape rate for experimental data has been demonstrated by Jolivet *et al*. (2006).

The term escape noise has been chosen in analogy to the Arrhenius formula which

https://doi.org/10.1017/CBO9781107447615.011 Published online by Cambridge University Press

describes the escape of a particle (or a chemical process) across an energy barrier in the presence of thermal energy (van Kampen, 1992).

The relation of diffusive noise in the input to escape noise has been studied by Plesser and Gerstner (2000), Herrmann and Gerstner (2001) and Mensi *et al*. (2011). Stochastic resonance has been a popular topic of research for many years, starting in 1989 (McNamara and Wiesenfeld, 1989; Douglass *et al*., 1993; Longtin, 1993; Collins *et al*., 1996). A nice review on stochastic resonance can be found in Gammaitoni *et al*. (1998).

Exercises

1. **Integrate-and-fire model with linear escape rates**. *Consider a leaky integrate-and-fire neuron with linear escape rate,*

$$\rho_I(t|\hat{t}) = \beta\,[u(t|\hat{t}) - \vartheta]_+. \tag{9.38}$$

(a) Start with the non-leaky integrate-and-fire model by considering the limit of $\tau_m \to \infty$. *The membrane potential of the model is then*

$$u(t|\hat{t}) = u_r + \frac{1}{C}\int_{\hat{t}}^{t} I(t')\mathrm{d}t'\,. \tag{9.39}$$

Assume constant input, set $u_r = 0$ *and calculate the hazard and the interval distribution.*

(b) Consider the leaky integrate-and-fire model with time constant τ *and constant input* I_0. *Determine the membrane potential, the hazard, and the interval distribution.*

2. **Likelihood of a spike train**. *In an in-vitro experiment, a time-dependent current* $I(t)$ *was injected into a neuron for a time* $0 < t < T$ *and four spikes were observed at times* $0 < t^1 < t^2 < t^3 < t^4 < T$.

(a) What is the likelihood that this spike train could have been generated by a leaky integrate-and-fire model with linear escape rate defined in Eq. (9.38)?

(b) Rewrite the likelihood in terms of the interval distribution and hazard of time-dependent renewal theory.

https://doi.org/10.1017/CBO9781107447615.011 Published online by Cambridge University Press